List of pdfcomments

AJR - 8
AJR - 8
AJR - 10
AJR - 10
AJR - 15

Modelling 3D turbulent floods based upon the Smagorinski large eddy closure

Meng Cao[1] and A. J. Roberts[1]

[1]School of Mathematical Sciences
University of Adelaide, South Australia 5005,
Australia

1 Abstract

Rivers, floods and tsunamis are often very turbulent. Conventional models of such environmental fluids are typically based on depth averaged inviscid irrotational flow equations. We explore the implications of changing the theoretical base to the turbulent Smagorinski large eddy closure. The aim is to more appropriately model the fluid dynamics of such complex environmental fluids by using such a turbulent closure. Large changes in fluid depth are allowed. Computer algebra constructs the slow manifold of the flow in terms of the fluid depth and the mean turbulent lateral velocities. The major challenge is to deal with the nonlinear stress tensor in the Smagorinski closure. The model integrates the effects of inertia, self-advection, bed drag, gravitational forcing and turbulent dissipation with minimal assumptions. Although the resultant model is close to established models, the real outcome is creating a sound basis for the modelling so others, in their

modelling of more complex situations, can systematically include more complex physical processes.

Keywords turbulent flood, tsunami, Smagorinski closure, channel flows

2 Introduction

Environmental turbulent fluids have large wave length compared with the fluid depth. Bousmar [1], Liu et al. [5], Demuren [3] and others experimentally and numerically explored compound channel flows as being typical of such environmental turbulent fluid. Conventional mathematical models of such flows are carried out by depth averaging the flow equations. Bousmar [1] proposed an exchange discharge model (EDM) by depth averaging the Navier–Stokes equations. The EDM solves the momentum transfers experimentally and numerically through the turbulent exchange and geometrical transfer between channel subsections, the channel and the shallow regions. The EDM predicts the discharge and water profile computation successfully and supports our simulations of flows along straight channels. Liu et al. [5] simulated shallow water flows in curved and meandering channels by a depth averaged lattice Boltzmann model by using the large eddy simulation model to account for turbulence. Our simulations of flows over meandering channels are compared with those of Liu et al. [5].

However, Roberts [8] discussed evidence that the depth averaging in such models is quantitatively unsound. Here we resolve some of the turbulent dynamics using the Smagorinski model. But instead of depth averaging flow equations, we obtain low order models based upon centre manifold theory. The theory assures that there exists an emergent low dimensional, slow manifold for the evolution governed by the continuity equation (1), momentum equation (2) and nonlinear shear tensor in the Smagorinski closure (7). The resulting model is then used to simulate flows

over straight and meandering compound channels and to compare with published data [1, 5, e.g.].

3 Detailed equations of the turbulent model

Let's consider three dimensional incompressible and irrotational turbulent fluid flowing down a slightly sloping ground. Define Cartesian coordinates with the lateral directions $x_1 = x$ and $x_2 = y$ and the normal direction $x_3 = z$. Let the turbulent fluid have thickness $h(x, y, t)$ over the ground located at $z = b(x, y)$ with a mean slope θ in the $x = x_1$ direction, denote the turbulent mean velocity field by $\boldsymbol{q}(x, y, z, t) = (u, v, w) = (u_1, u_2, u_3)$, and the turbulent mean pressure field by $p(x, y, z, t)$. After non-dimensionalising the variables with respect to a typical fluid thickness H, the velocity scale $\sqrt{gH}$, and the fluid density, the non-dimensional governing partial differential equations for the incompressible, irrotational, three dimensional, turbulent mean fluid fields are the continuity equation

$$\boldsymbol{\nabla} \cdot \boldsymbol{q} = \frac{\partial u}{\partial x} + \frac{\partial v}{\partial y} + \frac{\partial w}{\partial z} = 0 \,, \tag{1}$$

and the momentum equation

$$\frac{\partial \boldsymbol{q}}{\partial t} + \boldsymbol{q} \cdot \boldsymbol{\nabla} \boldsymbol{q} = -\boldsymbol{\nabla} p + \boldsymbol{\nabla} \cdot \tau + \boldsymbol{g} \,, \tag{2}$$

where τ is the turbulent mean stress tensor, and $\boldsymbol{g} = (g_1, 0, g_3)$ is the forcing from gravity ($|\boldsymbol{g}| = 1$ by the non-dimensionalisation). In the Smagorinski model the effects of turbulence are modelled by via an eddy viscosity ν, which is related to the mean shear stress through the mean stress-strain equation of

$$\tau_{ij} = 2\nu \dot{\varepsilon}_{ij} \,, \tag{3}$$

with the indexes $i, j = 1, 2, 3$ indicating in the x, y and z directions. Define the turbulent mean strain-rate tensor [10, 4, e.g.]

$$\dot{\varepsilon}_{ij} = \frac{1}{2}\left(\frac{\partial u_i}{\partial x_j} + \frac{\partial u_j}{\partial x_i}\right), \tag{4}$$

and then the non-dimensional turbulent mean stress tensor for the turbulent fluid is

$$\sigma_{ij} = -p\delta_{ij} + 2\nu\dot{\varepsilon}_{ij}\,. \tag{5}$$

When the eddy viscosity ν is constant, equation (5) models a Newtonian fluid. In the Smagorinski model [7, e.g.], the eddy viscosity ν varies linearly with the magnitude $\dot{\varepsilon}$ of the second invariant of the strain-rate tensor,

$$\nu = c_t h^2 \dot{\varepsilon} \quad \text{where} \quad |\dot{\varepsilon}|^2 = \sum_{i,j} \dot{\varepsilon}_{ij}^2\,. \tag{6}$$

Roberts et al. [10] recommended the proportionality constant $c_t \approx 0.02$ for turbulent environmental flows through comparison with established channel flow experiments [6, e.g.]. Thus, equations (3)–(6) give the turbulent mean stress tensor

$$\tau_{ij} = 2\nu(\dot{\varepsilon})\dot{\varepsilon}_{ij} = c_t h^2 \dot{\varepsilon}\left(\frac{\partial u_i}{\partial x_j} + \frac{\partial u_j}{\partial x_i}\right). \tag{7}$$

We formulate boundary conditions on the ground $z = b(x, y)$ and free surface $z = \eta(x, y, t) = h(x, y, t) + b(x, y)$ in terms of the turbulent mean velocity field $\boldsymbol{q}(x, y, z, t)$ and the fluid depth $h(x, y, t)$. On the ground, no fluid penetrating the ground requires $\boldsymbol{q} \cdot \boldsymbol{n} = 0$:

$$w = ub_x + vb_y \quad \text{on } z = b\,, \tag{8}$$

where the unit normal vector to the ground is

$$\boldsymbol{n} = (-b_x, -b_y, 1)/\sqrt{1 + b_x^2 + b_y^2}. \tag{9}$$

We posit a slip law on the ground to account for a negligibly thin turbulent boundary layer:

$$\boldsymbol{q}_{\tan} = c_u h \frac{\partial \boldsymbol{q}_{\tan}}{\partial n} \quad \text{on } z = b\,, \tag{10}$$

where $\boldsymbol{q}_{\tan}$ represents the velocity tangential to the ground. Roberts et al. [10] found the constant $c_u \approx 1.85$ matched open channel flow observations. In a wider range of applications, the coefficient c_u would change for different ground roughness. Unit vectors tangential to the ground in the x and y directions are

$$\boldsymbol{t}_x = \frac{1}{\sqrt{1+b_x^2}}(1,0,b_x) \quad \text{and} \quad \boldsymbol{t}_y = \frac{1}{\sqrt{1+b_y^2}}(0,1,b_y).$$

The boundary condition (10) on the ground $z = b$ becomes

$$\frac{1}{\sqrt{1+b_x^2}}(u + wb_x) = \frac{c_u h}{\sqrt{1+b_x^2+b_y^2}} \frac{\partial}{\partial n}(u + wb_x)\,, \tag{11}$$

$$\frac{1}{\sqrt{1+b_y^2}}(v + wb_y) = \frac{c_u h}{\sqrt{1+b_x^2+b_y^2}} \frac{\partial}{\partial n}(v + wb_y)\,. \tag{12}$$

On the free surface (that is, on its turbulent mean position), the kinematic condition is

$$\frac{\partial \eta}{\partial t} + u\frac{\partial \eta}{\partial x} + v\frac{\partial \eta}{\partial y} = w \quad \text{on } z = \eta = h + b\,, \tag{13}$$

Relative to atmospheric pressure, the pressure on the free surface is zero. Thus the turbulent mean stress normal to the free surface is also zero: on $z = \eta$,

$$-p + \frac{\tau_{33} - 2\eta_x\tau_{13} - 2\eta_y\tau_{23} + \eta_x^2\tau_{11} + 2\eta_x\eta_y\tau_{12} + \eta_y^2\tau_{22}}{1+\eta_x^2+\eta_y^2} = 0\,. \tag{14}$$

There must be no turbulent mean, tangential stress at the free surface: namely the following for the case of parameter $\gamma = 1$,

$$(1-\eta_x^2)\tau_{13} + \eta_x(\tau_{33} - \tau_{11}) - \eta_y(\tau_{12} + \eta_x\tau_{23})$$

$$= \frac{(1-\gamma)\sqrt{2}c_t}{(1+c_u)(1+2c_u)} u\sqrt{u^2+v^2} \quad \text{on } z=\eta\,, \tag{15}$$

$$(1-\eta_y^2)\tau_{23} + \eta_y(\tau_{33}-\tau_{22}) - \eta_x(\tau_{12}+\eta_y\tau_{13})$$

$$= \frac{(1-\gamma)\sqrt{2}c_t}{(1+c_u)(1+2c_u)} v\sqrt{u^2+v^2} \quad \text{on } z=\eta\,. \tag{16}$$

4 Reduced model of the fluid dynamics

This section focusses on interpreting the application of centre manifold theory and the resulting modelling of the turbulent flow. Instead of depth averaging equations, we apply centre manifold theory to deal with the turbulent dynamics across the fluid layer. Roberts, Georgiev and Strunin [10, 4] detailed similar approaches by introducing the parameter γ into the free surface tangential stress conditions (15) and (16) where $\gamma = 0$ empowers analytic analysis and approximation, whereas $\gamma = 1$ recovers the physical case. As described in previous research [10, 4], when parameter $\gamma = 0$ lateral shear modes of turbulent flow become neutral modes of the dynamics, that is, they form a slow subspace along with conservation of fluid. Centre manifold theory [12, e.g.] then assures us that there exists a slow manifold, that we can construct, of the nonlinear dynamics and under changes in the parameters. Evaluating the resulting slow manifold model at the real case of parameter $\gamma = 1$ then provides a model for the fluid dynamics.

Roberts [9], in a freely available report, detailed the computer algebra that constructed the slow manifold model in 2D flow. Modifications for 3D flow empowers the computer algebra program to derive the evolutions of the water depth $h(x,y,t)$ and the depth averaged lateral velocities $\bar{u}(x,y,t)$ and $\bar{v}(x,y,t)$. In the centre manifold framework we can choose any reasonable measure of the fluid dynamics in order to parametrise the model: we *choose* the depth averaged lateral velocities and fluid depth.

We let $\bar{q}(x,y,t) = \sqrt{\bar{u}^2 + \bar{v}^2}$ denote the depth averaged speed of the fluid flow. Omitting the intricate details of the derivation, the evolution of $h(x,y,t)$, $\bar{u}(x,y,t)$ and $\bar{v}(x,y,t)$ are described by the fluid conservation equation and by effective lateral momentum equations:

$$\frac{\partial h}{\partial t} \approx -\frac{\partial h\bar{u}}{\partial x} - \frac{\partial h\bar{v}}{\partial y}\,, \tag{17}$$

$$\begin{aligned}\frac{\partial \bar{u}}{\partial t} \approx\ & -0.00293\frac{\bar{u}\bar{q}}{h} + 0.993\left(g_x - g_z\frac{\partial h}{\partial x} - g_z\frac{\partial b}{\partial x}\right) \\ & - 1.030\bar{v}\frac{\partial \bar{u}}{\partial y} - 1.045\bar{u}\frac{\partial \bar{u}}{\partial x} - 0.0115\bar{u}\frac{\partial \bar{v}}{\partial y} + 0.0136\bar{v}\frac{\partial \bar{u}}{\partial y} \\ & + 0.0030\bar{u}\frac{\partial \bar{v}}{\partial y} + 0.0204\bar{u}\frac{\partial \bar{u}}{\partial x} + 0.237h\bar{q}\frac{\partial^2 \bar{u}}{\partial y^2} + 0.0266h\bar{q}\frac{\partial^2 \bar{u}}{\partial x^2}\,,\end{aligned} \tag{18}$$

$$\begin{aligned}\frac{\partial \bar{v}}{\partial t} \approx\ & -0.00293\frac{\bar{v}\bar{q}}{h} - 0.993g_z\left(\frac{\partial h}{\partial y} + \frac{\partial b}{\partial y}\right) - 1.042\bar{v}\frac{\partial \bar{v}}{\partial y} \\ & - 1.026\bar{u}\frac{\partial \bar{v}}{\partial x} + 0.0037\bar{u}\frac{\partial \bar{u}}{\partial y} - 0.0152\bar{v}\frac{\partial \bar{u}}{\partial x} + 0.0167\bar{v}\frac{\partial \bar{v}}{\partial y} \\ & + 0.0097\bar{u}\frac{\partial \bar{v}}{\partial x} - 0.0038\bar{u}\frac{\partial \bar{u}}{\partial y} + 0.0068\bar{v}\frac{\partial \bar{u}}{\partial x} \\ & + 0.249h\bar{q}\frac{\partial^2 \bar{v}}{\partial y^2} + 0.0060h\bar{q}\frac{\partial^2 \bar{v}}{\partial x^2} + 0.256h\bar{q}\frac{\partial \bar{u}}{\partial x}\frac{\partial \bar{u}}{\partial y}\,.\end{aligned} \tag{19}$$

Equations (17)–(19) are a result of taking into account the relatively slow variations in the lateral directions x and y via small but non-zero lateral derivatives ∂_x and ∂_y. They are a form of slowly varying approximations [8, e.g.]. The momentum equations (18) and (19) incorporate inertial terms $\bar{\boldsymbol{q}}_t$, self-advection terms $\bar{\boldsymbol{q}}\partial\bar{\boldsymbol{q}}/\partial x$, ved drag terms $\bar{q}\bar{\boldsymbol{q}}/h$, gravitational forcing $g_x - g_z\boldsymbol{\nabla}(h+b)$, and other terms related to the turbulent mixing, where $\bar{\boldsymbol{q}} = (\bar{u},\bar{v})$. Although equations (17)–(19) are expressed in terms of depth averaged lateral velocities, they are derived not by depth averaging, but instead by systematically accounting for interaction between vertical profiles of the velocity

and the stress and bed drag and lateral space variations. The form and coefficients in equations (17)–(19) are supported by dynamical systems theory: the detail in the equations reflects that a slow manifold is in principle composed of exact solutions of the full dynamics and hence accounts for all interactions up to a given order of analysis no matter how small the numerical coefficient in the interactions.

In practice one might only implement those terms of equations (17)–(19) which are important in a specific application. Future planned research is to explore how important is each of the multitude of terms in some flows of environmental interest. Our first task here is then to establish the model's predictions in a range of turbulent flows.

5 Modelling flows along straight channels

This section focuses on the preliminary application of the model (17)–(19) for turbulent flow driven by a small downslope along straight open channels. The water covers the entire domain in order to avoid, at this stage, complications of moving contact lines between wet and dry bed: the flow is in the channel and over a surrounding flood plain. We compare this turbulent channel flow with viscous open channel flow by Roberts et al. [11] and the experiments of turbulent flow over flood plains and channels in a flume with water of variable depth by Bousmar et al. [1, 2].

Let x be the down-stream and y be the cross-stream coordinate. We choose a quartic shape for the channel to make smooth transitions to and from the shallows and the channel:

$$z = b(x, y) = -1 + B - B\left\{\max\left[0, 1 - (y/\beta)^2\right]\right\}^2, \qquad (20)$$

where β denotes the half-width of the channel, $1 - B$ the depth of water on the shallow 'flood plain' on either side of the channel, and the mid-depth of the channel is one (non-dimensionally) as

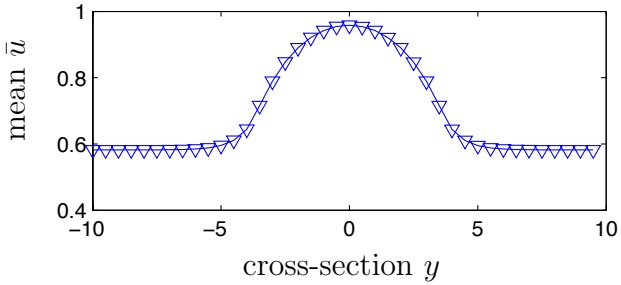

Figure 1: Plot of the mean downstream velocity $\bar{u}$ in the cross-section at the point $x = 20$ and the time $t = 800$ with parameters $2\beta = 8$, $B = 0.9$ and $\theta = 0.01$. The channel is nine times as deep as in the surrounding shallows, but the peak downstream velocity is only 50% faster than in the shallows.

we set the mean water level to be at $z = 0$. For the simulations reported here we set $2\beta = 8$, $B = 0.9$ so the shallows are of depth 0.1, and a mean slope $\theta = 0.01$ in the x direction. For comparison, the channel of Bousmar [1] was about twice as deep in the constant channel as in the flood plain.

Numerical simulations were simply implemented using centred difference approximations to the spatial derivatives in equations (17)–(19) on a regular but staggered grid in space. Time integration was performed by Matlab's `ode15s`.

In simulations, we typically started the fluid with zero velocity and a flat free surface ($z = 0$). Transients in the simulations decayed on a non-dimensional time of typically $t = 400$. Figure 1 shows that fast flow developed in the deeper channel and slow flow on the shallow regions. In a viscous flow in a small open channel [11], the flow was eight times as fast in the channel as on the shallow regions. Equation (18) suggests the equilibrium downstream velocity in the shallow regions is $\sqrt{0.993 \sin(0.01) \times 0.1/0.00293} \approx 0.58$, which corresponds the numerical result in Figure 1. The equilibrium downstream velocity for a fluid of depth one is $\sqrt{0.993 \sin(0.01) \times 1/0.00293} =$

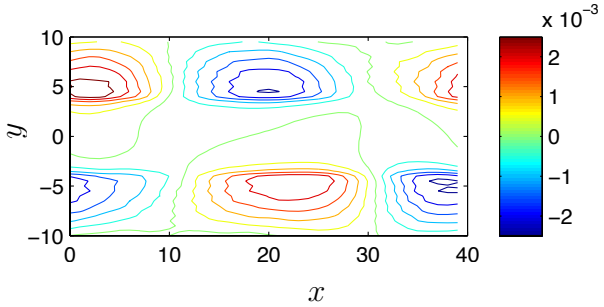

Figure 2: Contours of the mean transverse velocity $\bar{v}$ at time $t = 800$ with parameters $2\beta = 8$, $B = 0.9$ and $\theta = 0.01$. The high value curves (red) and low value curves (blue) indicate travelling vortices on the shear near the interactions between the channel and shallow regions.

1.84, but in our channel is only 0.95 as in Figure 1: such simulations show that when the shape of the bed becomes complex, the equilibrium downstream velocity decreases through lateral mixing and dissipation. For example, for the lesser slope $\theta = 0.001$, the equilibrium downstream velocity over a flat bed is 0.58, in mid-channel with width $2\beta = 14$ is 0.37, in mid-channel with width $2\beta = 8$ is 0.30, and in a slightly meandering channel with a width $2\beta = 8$ is 0.31. Figure 2 displays the contour of the mean transverse velocity $\bar{v}(x, y, t)$ at time $t = 800$, which indicates that weak horizontal vortices grow on the shear in the transition between the channel and shallow regions. These weak mixing vortices travel downstream. Similar vortices were observed by Roberts and Li [11] in numerical simulations of viscous open channel flow and by Boussmar [2] in experiments of turbulent flow along channels in a flume.

6 Flows along meandering channels

This section describes simulations of turbulent flow over a slightly sloped ground with a meandering open channel. The simulations are compared with the numerical results of Liu et al. [5] and Demuren [3] who calculated the two and three dimensional turbulence flows in meandering channels by a lattice Boltzmann model and a finite volume numerical model, respectively.

Here we describe simple meandering open channels by the bed

$$z = b(x, y) = -1 + B - B \left\{ \max \left[0, 1 - \left(\frac{y - \kappa_1 \cos(\kappa_2 x)}{\beta} \right)^2 \right] \right\}^2 , \tag{21}$$

where the parameter κ_2 determine the wavelength $2\pi/\kappa_2$ of the meandering channel, the parameter κ_1 is the half-width of the extent of the meanders, and the parameters β and $1 - B$ are the half-width and mid-depth of the meandering channel as before. Simulate the turbulent flow over such channel by the equations (17)–(19) with periodic boundary conditions in both x and y directions for both the flow and channel.

In our numerical simulations, we found transients decay over times of typically $t \approx 400$. Figure 3 exhibits the contours of the depth averaged lateral velocities $\bar{u}(x, y, t)$ and $\bar{v}(x, y, t)$. The downstream velocity $\bar{u}$ reaches maximum at the bends. The transverse velocity $\bar{v}$ attains maximum and minimum at the connection of the bends, which is consistent with the results of Liu eta al. [5] who modelled the water in meandering channels with 60° and 90° consecutive bends and a width of 0.3 m. Demuren [3] calculated the water depth and the depth averaged longitudinal and transverse velocities of three dimensional flows in meandering channels with a natural bed configuration by a finite volume numerical method. Simulations at fifteen observed stations of the meandering channel indicate that the location of

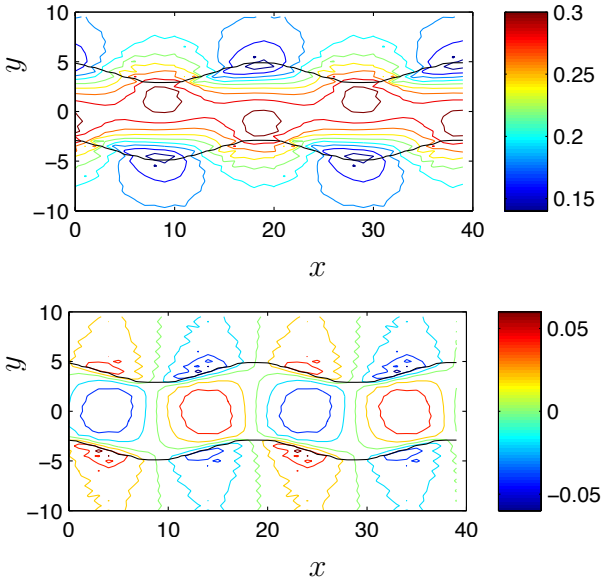

Figure 3: Contours of the mean downstream velocity $\bar{u}$ (top) and mean transverse velocity $\bar{v}$ (bottom) at time $t = 800$ with parameters $2\beta = 8$, $B = 0.9$, $\theta = 0.01$, $\kappa_1 = 1$ and $\kappa_2 = 4\pi/L_x$. The black curves plot the meandering channel.

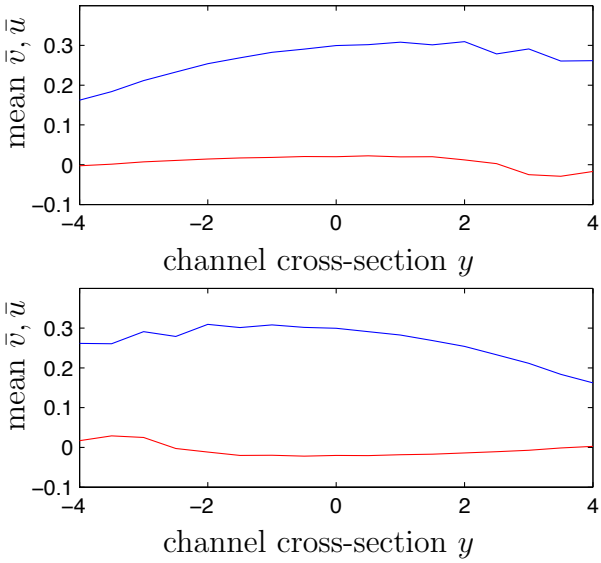

Figure 4: The mean downstream velocity $\bar{u}(x, y, t)$ (blue) and the mean transverse velocity $\bar{v}(x, y, t)$ (red) in the cross-section of the channel at the bend $x = 10$ (top) and $x = 20$ (bottom). The relevant parameters $2\beta = 8$, $B = 0.9$, $\theta = 0.01$, $\kappa_1 = 1$ and $\kappa_2 = 4\pi/L_x$.

the maximum velocity shifts from the inner bank to the outer bank as the water flows through the bends of the channel.

Plots of the water depth do not show any features of much interest: plots are dominated by the variations in the bed. Figure 4 plots of the the downstream velocity $\bar{u}(x, y, t)$ and the transverse velocity $\bar{v}(x, y, t)$ at the channel bends $x = 10$ and $x = 20$. The downstream velocity and transverse velocity are bigger in the outer bank than in the inner bank, which correspond to the computations by Demuren [3].

7 Conclusion

The proposed approach to supporting turbulent flood models by the dynamical systems theory of centre manifolds appears to predict environmental turbulent fluids reliably. The flows in straight and meandering compound channel, as examples, were numerically simulated by the new approach. The results correspond to the analysis and numerical simulations of the published work [1, 5, e.g.]. The equations (17)–(19) account for the interactions between the vertical profiles and lateral spatial variations, and thus may in future work be used to better model erosion and sediment transport of the turbulent fluid.

References

[1] Bousmar, D., *Flow modelling in compund channels: momentum trans- fer between main channel and prismatic and non-prismatic floodplains*, Ph.D. thesis, Universitie Catholique de Louvain, 2002.

[2] Bousmar, D. and Zech, Y., Large-scale coherent structures in compound channels, Technical report, Universitie Catholique de Louvain, 2003.

[3] Demuren, A. O., A numerical model for flow in meandering channels with natural bed topography, *Water*, **29**, 1993, 1269.

[4] Georgiev, D. J., Roberts, A. J. and Strunin, D. V., Modelling turbulent flow from dam break using slow manifolds, in *Proceedings of the 14th Biennial Computational Techniques and Applications Conference, CTAC-2008*, editors G. N. Mercer and A. J. Roberts, 2009, volume 50 of *ANZIAM J.*, C1033–C1051, C1033–C1051, http://journal.austms.org.au/ojs/index.php/ANZIAMJ/article/view/1466.

[5] Liu, H., Zhou, G. J. and Burrows, R., Lattice boltzmann model for shallow water flows in curved and meandering channels, *International Journal of Computational Fluid Dynamics*, **23**, 2009, 209–220.

[6] Nezu, I., Open-channel flow turbulence and its research prospect in the 21st century, *J. Hydraulic Engineering*, **131**, 2005, 229–246.

[7] Ozgokmen, T. M., Iliescu, T., Fisher, P. F., Srinivasan, A. and Duan, J., Large eddy simulation of stratified mixing in two-dimensional dam-break problem in a rectangular enclosed domain, *Ocean Modelling*, **16**, 2007, 106–140.

[8] Roberts, A. J., Low-dimensional models of thin film fluid dynamics, *Phys. Letts. A*, **212**, 1997, 63–72, doi:10.1016/0375-9601(96)00040-0.

[9] Roberts, A. J., Computer algebra describes flow of turbulent floods via the smagorinski large eddy closure, Technical report, University of Southern Queensland, 2008, http://eprints.usq.edu.au/4008/.

[10] Roberts, A. J., Georgiev, D. J. and Strunin, D. V., Model turbulent floods with the Smagorinsky large eddy closure, Technical report, http://arxiv.org/abs/0805.3192, 2008.

[11] Roberts, A. J. and Li, Z., An accurate and comprehensive model of thin fluid flows with inertia on curved substrates, *J. Fluid Mechanics*, **553**, 2006, 33–73, doi:10.1017/S0022112006008640.

[12] Vanderbauwhede, A. and Iooss, G., Center manifold theory in infinite dimensions, *Dynamics Reported*, **1**, 1988, 125–163.